Random wave methods for the prediction of the RCS of homogeneous chaotic straight ducts.

Andrew Mackay

DERA Malvern, St Andrew's Road
Great Malvern, Worcs WR14 3PS, UK

Ref no: DERA/S&E/RAD/JP010450

February 2001

Abstract

It is now fairly well established that convergence of shooting-and-bouncing (SBR) ray methods is not feasible for the determination of radar cross section (RCS) of most realistic engine ducts. This is a consequence of classical chaos theory which was not recognised by radar engineers until quite recently (Mackay 1998). However, at the time no solution to the problem was offered. In this paper a random wave method is described for the determination of representative RCS distributions of chaotic straight ducts, under two assumptions; (1) that there is local field homogeneity, (2) that a Kirchhoff approximation is valid. Typical duct field magnitudes are illustrated for a stadium cross section duct and the RCS is predicted as a function of scatter angle. A comparison is also made with an accurate modal solution.

1.1 Introduction

Some recent findings are presented to explore the implications and applications of chaos theory to the high frequency Radar Cross Section (RCS) prediction of complex engine ducts. This is probably the first study of its kind and provides an unexpected link to an area of mathematical physics not traditionally viewed as relevant to radar scattering.

In previous work [1, 2, 3, 4], it is shown that the Deschamps [5] first order ray theory can be reformulated in terms of a compound deviation matrix related to a Poincaré surface of section; a fact which is not well known to radar engineers. Chaos theory shows that, for all but the simplest problems with high symmetry, curved ducts will amplify any error in the initial ray trajectory exponentially with the number of ray bounces. The average rate of exponential growth is characterised by the Lyapunov exponent which can be calculated directly from the compound deviation matrix, or the average ray divergence. An important consequence is that it becomes computationally impossible to accurately (in a point-wise sense) predict the RCS of even quite simple duct structures using shooting-and-bouncing (SBR) methods.

What strategies may be adopted? One could abandon high frequency ray-based methods in an attempt to predict RCS using accurate numerical boundary element, finite element or FDTD (finite difference time domain) methods. This may actually be feasible with recent advances in FMM (fast multi-level multipole methods) [6], though the computer power required is still formidable for ducts whose surface area is many hundreds of thousands of square wavelengths. However, there is still a very important requirement for high frequency asymptotic methods. In recent years, much of the necessary mathematics has been developed for application to related problems in quantum mechanics.

It is suggested that at high frequencies it is unnecessary to require the exact solution to Maxwell's equations on a given duct boundary. Indeed, even if a convergent geometrical optics solution were obtained this would not represent such a solution. It is more important to obtain a low complexity method which accurately predicts the important RCS *statistics* such as the mean, standard deviation and lobing rate. The determination of the correct electric field and RCS statistics on a general chaotic duct is a difficult and currently unsolved problem in chaos theory. Even for straight ducts, whose cross section is constant, the general case includes *soft* or *mixed* chaos [7] where the field is not homogeneous on a duct section. Recent work, involving random matrix theory, has begun to address this problem (e.g. [8, 9]) but the subject is not mature.

In order to discuss statistics it is first necessary to define the ensemble over which the statistics are generated. For chaotic ducts it will be assumed that the ensemble is the class of all ducts whose geometry does not differ significantly from a reference geometry in terms of relative duct dimensions, but whose perturbations from the reference geometry are large compared to a wavelength. Thus in the high frequency limit the changes in the relative duct dimensions necessary to characterise the ensemble can be arbitrarily small. Only if the RCS statistics are slowly varying functions of angle of incidence

is it justified to replace this ensemble by an ensemble over angles of incidence, under an assumption of local ergodicity [10, section 2.2.2].

In the model presented it is assumed that the scattered field at the exit plane of the duct can be represented as the sum of a chaotic homogeneous "random wave" field and a convergent SBR contribution. The effect of "scarring" from the contribution of short rays [11] is assumed to be accounted for by the convergent SBR term. It is likely that this may be a useful model for quite a large class of chaotic straight ducts.

1.2 A random wave representation for a uniform straight ducts

A uniform straight duct (henceforth termed a straight duct) is defined as one whose axis is a straight line and whose cross section is independent of position down the axis. Only perfectly conducting ducts will be considered here, terminated by a perfectly conducting plane orthogonal to the duct axis. Under mirror symmetry, a terminated duct of length L can be unfolded as an open-ended duct of length $2L$ with the exit aperture made distinct from the entry aperture. This is illustrated in figure 1, where ξ_{in} refers to the off-axis angle and ϕ_{in} refers to the azimuthal angle of an incident plane wave. Such a plane wave is decomposed as a set of ray bundles with identical directions under the SBR method.

In the random wave representation, it is assumed that all knowledge of the transverse ray direction (the projection of a ray on to a plane perpendicular to the axis) is lost. Thus the field is represented by a sum of plane waves whose phase and transverse direction are random. On the other hand, the angle θ_{in} that a ray makes with the duct axis is a constant of the motion of a ray in a straight duct. In the SBR method it is assumed that $\theta_{in} = \xi_{in}$. More accurate methods, such as the "generalised ray expansion" (GRE) [12, 4] require a decomposition of the incident field as a spectrum of ray bundles due to the finite size of the aperture. In this case energy is carried by rays for which $\theta_{in} \neq \xi_{in}$.

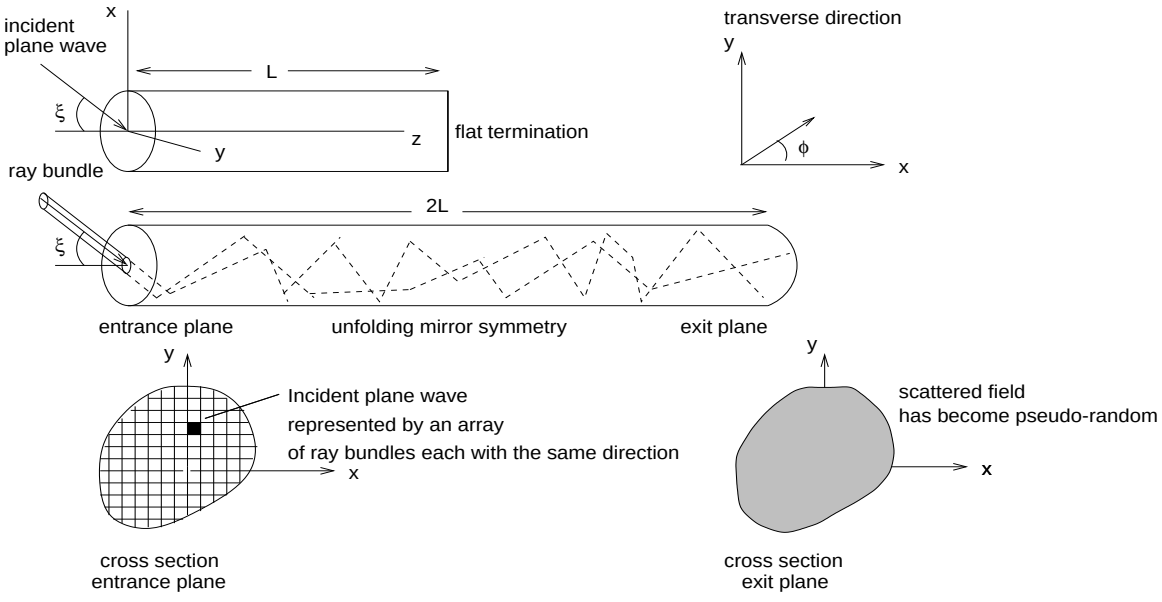

Figure 1. *Unfolding a straight duct with flat termination*

For each plane wave component, the polarisation is fixed and dependent on the polarisation of the incident wave. There are two orthogonal incident wave polarisations whose electric field lies in the direction of increasing ϕ_{in} and in the direction of increasing ξ_{in} which can be treated separately. In the model the magnitude of each plane wave component is assumed to be equal. This is convenient because it represents a numerical implementation of the SBR model in the case where first order rays are relegated to zero order rays with bundle size equal to the duct cross section. A Gaussian distribution of amplitudes provides an alternative model. When the number of plane wave components, M, is sufficiently large there is expected to be negligible difference between the equal-amplitude and Gaussian models, provided they are both suitably normalised with respect to transmitted power.

Suppose that an SBR method is employed for which a significant number (possibly all) the ray bundles have diverged unacceptably. This number will depend on the convergence threshold, the number of ray bundles traced, the angle of incidence of the incident plane wave, the length of the duct and the cross section geometry. Suppose this number is N_B and that the total number of launched ray bundles is N_{tot}. The ray contribution to the transverse aperture field on the exit aperture, carried by the N_B diverged rays, is then replaced by a transverse contribution, $\boldsymbol{E}_{r,\perp}$. For an incident plane wave with fixed angle of incidence, the transverse duct field can thus be modelled as,

$$\boldsymbol{E}_{r,\perp}(x,y) \equiv E_{r,x}\hat{\boldsymbol{x}} + E_{r,y}\hat{\boldsymbol{y}} = A_2 \sum_{l=1}^{M} \boldsymbol{p}_{\perp,l} e^{-j[k_0 \sin\xi(x\cos a_l + y \sin a_l) + b_l]} \tag{1}$$

for independent random variables a_l and b_l, uniformly distributed over the interval 0 to 2π. The polarisation $\boldsymbol{p}_{\perp,l}$ is defined by,

$$\boldsymbol{p}_{\perp l} = \begin{cases} -\sin a_l \hat{\boldsymbol{x}} + \cos a_l \hat{\boldsymbol{y}} & \hat{\boldsymbol{\theta}} \text{ inc. polzn.} \\ (\cos a_l \hat{\boldsymbol{x}} + \sin a_l \hat{\boldsymbol{y}}) \cos\xi & \hat{\boldsymbol{\xi}} \text{ inc. polzn.} \end{cases} \tag{2}$$

for the two different states of incident polarisation. The normalisation constant A_2 is defined by,

$$A_2 = \sqrt{\frac{N_B}{M N_{tot}}} \tag{3}$$

With the exit aperture field known, it is straight forward to determine the far-field via a near-to-far field transformation (e.g. [13]), and hence the RCS, assuming a standard Kirchhoff approximation. In particular it is assumed that the true scattered field on the original duct prior to unfolding is equal to the field on the exit aperture on the unfolded duct. This ignores the effect of multiple reflections within the duct, the detailed structure of the duct lip and features external to the duct.

Suppose an observer is situated at a point distant from the duct at an elevation angle ξ_s and azimuth angle ϕ_s measured from the (x, y) origin of the duct exit plane. Thus ξ_s is the scatter angle between the line to the observer and the duct axis and ϕ_s is the scatter angle between the projection of this line on to the exit plane and the x-axis. Let $\hat{\boldsymbol{\xi}}_s$ and $\hat{\boldsymbol{\phi}}_s$ represent unit direction vectors in the directions of increasing angles. If the distance between the observer and the exit plane is r_s, then in the limit as

$r_s \to \infty$, the electric field at the observation point can be written as [13],

$$\widetilde{\boldsymbol{E}}_s(\xi_s, \phi_s) = \frac{e^{-jk_0 r_s}}{r_s}(E_{\xi s}\hat{\boldsymbol{\xi}}_s + E_{\phi s}\hat{\boldsymbol{\phi}}_s) \tag{4}$$

where

$$E_{\xi s}(\xi_s, \phi_s) = \frac{j}{\lambda}\iint_{\mathcal{D}}[E_x(x', y')\cos\phi_s + E_y(x', y')\sin\phi_s]e^{jk_0\sin\xi_s(x'\cos\phi_s + y'\sin\phi_s)}\,dx'\,dy' \tag{5}$$

$$E_{\phi s}(\xi_s, \phi_s) = \frac{-j}{\lambda}\cos\xi_s\iint_{\mathcal{D}}[E_x(x', y')\sin\phi_s - E_y(x', y')\cos\phi_s]e^{jk_0\sin\xi_s(x'\cos\phi_s + y'\sin\phi_s)}\,dx'\,dy' \tag{6}$$

and $\mathcal{D}$ is the domain of the exit aperture. In the case where $N_B = N_{tot}$, $E_x = E_{r,x}$ and $E_y = E_{r,y}$. More generally, E_x and E_y have coherent contributions from the converged ray field. $E_{\xi s}(\xi_s, \phi_s)$ and $E_{\phi s}(\xi_s, \phi_s)$ are the complex scattering coefficients in the $\hat{\boldsymbol{\xi}}_s$ and $\hat{\boldsymbol{\phi}}_s$ directions and $\lambda = 2\pi/k_0$ is the free space wavelength. Assuming a unit electric field incident plane wave, the bistatic radar cross section (RCS), polarised in the $\hat{\boldsymbol{\xi}}_s$ and $\hat{\boldsymbol{\phi}}_s$ directions, is defined by,

$$\begin{aligned}\sigma_{\xi s}(\xi_s, \phi_s) &= 4\pi|E_{\xi s}(\xi_s, \phi_s)|^2 \\ \sigma_{\phi s}(\xi_s, \phi_s) &= 4\pi|E_{\phi s}(\xi_s, \phi_s)|^2\end{aligned} \tag{7}$$

The RCS of a straight duct is characterised by an exit cone of angle $\xi_s = \pm\xi$ over which the RCS is a maximum. This is a special feature that results from the conservation of the angle ξ for any ray within the duct.

1.3 Angle of incidence variation

The model (1) assumes a plane wave with fixed incidence angle. Whereas (5) and (6) automatically determine scatter angle correlations, there is no mechanism to account for incidence angle correlation. A suitable generalisation can be constructed which has many of the features of a GRE. The transverse random electric field is represented in terms of a random scalar potential, $\psi_1(x, y)$ or $\psi_2(x, y)$, for an incident ξ (H-polarised) or ϕ (E-polarised) polarised plane wave, respectively. Thus,

$$\begin{aligned}\boldsymbol{E}^{(1)}_{r,\perp}(x, y) &= \hat{\boldsymbol{z}} \times \nabla_\perp\psi_1 \quad \text{(H-polarised)} \\ \boldsymbol{E}^{(2)}_{r,\perp}(x, y) &= \nabla_\perp\psi_2 \quad \text{(E-polarised)}\end{aligned} \tag{8}$$

where $\nabla_\perp \equiv \hat{\boldsymbol{x}}\partial/\partial x + \hat{\boldsymbol{y}}\partial/\partial y$. The scalar potentials are incidence angle correlated, by virtue of the finiteness of the aperture. Provided the Kirchoff approximation is valid, which requires $k_0 R_l \cos\xi_{in} \gg 1$ for an aperture with maximum inscribed circle of radius R_l, then one may construct,

$$\psi_{1,2}(x, y; \xi_{in}, \phi_{in}) = \int_0^{\pi/2} k_0^2\cos\xi'\sin\xi'\,d\xi' \int_{-\pi}^{\pi}\tilde{U}(\xi', \phi'; \xi_{in}, \phi_{in})\psi^{(U)}_{1,2}(x, y; \xi', \phi')\,d\phi' \tag{9}$$

where

$$\tilde{U}(\xi, \phi; \xi_{in}, \phi_{in}) = \iint_{\mathcal{A}} e^{-j[(k_x - k_0\sin\xi_{in}\cos\phi_{in})x + (k_y - k_0\sin\xi_{in}\sin\phi_{in})y]}dx\,dy \tag{10}$$

with the wave number components,

$$\begin{aligned}k_x &= k_0\sin\xi\cos\phi \\ k_y &= k_0\sin\xi\sin\phi\end{aligned} \tag{11}$$

The uncorrelated potentials, $\psi_1^{(U)}(x,y;\xi_{in},\phi_{in})$ and $\psi_2^{(U)}(x,y;\xi_{in},\phi_{in})$, are assumed to be mutually independent and uncorrelated random functions of ξ_{in} and ϕ_{in}, defined by

$$\psi_{1,2}^{(U)}(x,y;\xi_{in},\phi_{in}) = L^{(1,2)} \sum_{l=1}^{P} e^{-j[k_0 \sin\xi_{in}(x\cos\alpha_l(\xi_{in},\phi_{in})+y\sin\alpha_l(\xi_{in},\phi_{in}))+\beta_l(\xi_{in},\phi_{in})]} \tag{12}$$

where, for each distinct pair of incidence angles, $\alpha_l(\xi_{in},\phi_{in})$ and $\beta_l(\xi_{in},\phi_{in})$ are independent uncorrelated random variables taken from a uniform distribution over $[0,2\pi]$. The normalisation constants $L^{(1,2)}$ are defined by,

$$L^{(1)} = \frac{A_2}{-jk_0\sin\xi} \qquad L^{(2)} = \frac{A_2\cos\xi}{-jk_0\sin\xi} \tag{13}$$

where A_2 is defined in (3).

Equation (12) can be used to can be used to numerically generate a table of uncorrelated fields at angles (ξ_{in},ϕ_{in}), sampled sufficiently finely, for any given realisation of a possible field distribution. Given a particular angle of incidence, a weighted set of these tabulated fields may be constructed to evaluate the correlated field at (ξ_{in},ϕ_{in}). Various numerical approximations and Fourier transform methods can be used to provide rapid computation. For example, (9) can be transformed to an integral over wavenumber space where it can be computed using an FFT. Also, provided the aperture does not differ significantly from a circle of average radius R_{av}, it is possible to approximate (10) as,

$$\tilde{U}(\xi,\phi;\xi_{in},\phi_{in}) \approx 2\pi R_{av}^2 \frac{J_1(k_0 R_{av}\gamma)}{k_0 R_{av}\gamma} \tag{14}$$

where $J_1(X)$ is the Bessel function of order 1 and,

$$\gamma = \sqrt{\sin^2\xi + \sin^2\xi_{in} - 2\cos(\phi-\phi_{in})\,\sin\xi\sin\xi_{in}} \tag{15}$$

Making a change in variable $\phi_{in}-\phi\to\phi$, the correlated potential may be written as,

$$\psi_{1,2}(x,y;\xi_{in},\phi_{in}) = \int_0^{\pi/2} k_0^2\cos\xi\sin\xi\,d\xi \int_{-\pi}^{\pi} 2\pi R_{av}^2 f_0(\xi,\phi;\xi_{in})\psi_{1,2}^{(U)}(x,y;\xi,\phi_{in}-\phi)\,d\phi \tag{16}$$

where

$$f_0(\xi,\phi;\xi_{in}) = \frac{J_1(X_0)}{X_0}$$

$$X_0 = k_0\gamma_0 R_{av}$$

and

$$\gamma_0 = \sqrt{\sin^2\xi + \sin^2\xi_{in} - 2\sin\xi\sin\xi_{in}\cos\phi} \tag{17}$$

In this method the effects of symmetry planes must be built in as an extra feature. For an aperture possessing no planes of mirror symmetry the above system can be used "as is". If there are symmetry planes then one can construct a correlated symmetric field as the correct symmetry preserving superposition of non-symmetric fields. The superposition is slightly different depending on the incident polarisation. It is possible to show that, if the x and y axes are both mirror planes, a symmetrised

transverse field for the H and E-polarised waves may be respectively represented by,

$$
\begin{aligned}
2\boldsymbol{E}_{r,\perp}^{\mathcal{R}_2,(1)}(\phi_{in};x,y) &= \boldsymbol{E}_{r,\perp}^{(1)}(\phi_{in};x,y) + \begin{pmatrix} -1 & 0 \\ 0 & 1 \end{pmatrix} \boldsymbol{E}_{r,\perp}^{(1)}(-\phi_{in};x,-y) \\
&+ \begin{pmatrix} 1 & 0 \\ 0 & -1 \end{pmatrix} \boldsymbol{E}_{r,\perp}^{(1)}(\pi-\phi_{in};-x,y) \\
&+ \begin{pmatrix} -1 & 0 \\ 0 & -1 \end{pmatrix} \boldsymbol{E}_{r,\perp}^{(1)}(\pi+\phi_{in};-x,-y) \\
2\boldsymbol{E}_{r,\perp}^{\mathcal{R}_2,(2)}(\phi_{in};x,y) &= \boldsymbol{E}_{r,\perp}^{(2)}(\phi_{in};x,y) + \begin{pmatrix} 1 & 0 \\ 0 & -1 \end{pmatrix} \boldsymbol{E}_{r,\perp}^{(2)}(-\phi_{in};x,-y) \\
&+ \begin{pmatrix} -1 & 0 \\ 0 & 1 \end{pmatrix} \boldsymbol{E}_{r,\perp}^{(2)}(\pi-\phi_{in};-x,y) \\
&+ \begin{pmatrix} -1 & 0 \\ 0 & -1 \end{pmatrix} \boldsymbol{E}_{r,\perp}^{(2)}(\pi+\phi_{in};-x,-y)
\end{aligned}
\tag{18}
$$

The factor of 2 is included to ensure a correct normalisation of power, since the square magnitudes of the fields are dominated by the trace terms. The x and y components of the symmetrised fields can then be used within the integrands of (5) and (6) to determine the symmetrised scattering coefficients.

1.4 Some examples

In the first example set an incident plane wave is assumed with fixed incidence angles, $\xi_{in} = 60^o$ and $\phi_{in} = 35^o$, polarised in the direction of increasing ϕ. It is also assumed that $N_B = N_{tot}$, i.e. that there is no ray-converged contribution to the RCS. A stadium cross section duct is considered, defined by two semi-circles of radius a smoothly joined to straight sections of length $a/2$. The wave number k_0 is defined by $k_0 a = 80.0$. The duct is assumed to be of length $2L = 30a$, for which an accurate modal solution [4, 14] using numerically determined eigenmodes has been obtained. The width of the maximum in the neighbourhood of ξ_s is inversely proportional to $k_0 a$.

Figures 2 and 3 illustrate the magnitude of the transverse field predicted using two members of the above random ensemble. Figure 4 shows the modal solution. Figures 5 and 6 illustrate the co-polar and cross-polar RCS on the exit cone, as a function of ϕ_s. The top curves show the co-polar RCS, where the scattered electric field is polarised in the direction of increasing ξ_s. The bottom curves show the cross-polar RCS, where the scattered electric field is polarised in the direction of increasing ϕ_s. These predictions should be compared with the reference modal solution in figure 7.

In the second example set the monostatic RCS is evaluated on the exit cone, where $\phi_s = \phi_{in}$ and $\xi_s = -\xi_{in} = 60^o$ (The "–" sign is required due to the reflection of coordinates in the mirror unfolding of the original terminated duct). Here, the incident wave is polarised in the direction of increasing ξ. (In the random wave model there is no distinction to be made between co-polar ξ or ϕ predictions. Cross-polar RCS differs by a constant factor of $\cos^4 \xi_{in}$.) Figures 8 and 9 show two random ensemble members illustrating the co-polar (top graph) and cross-polar (bottom graph) RCS as a function of ϕ_{in}. Figure 10 shows the predicted RCS from the modal solution. The random wave predictions show the correct mean RCS and short range angular correlation. There does, however, appear to be some evidence for longer range co-polar structure on the exit cone that is *not* modelled by the random wave monostatic predictions. At present the origin of these differences is uncertain.

1.5 Conclusions

A random wave model is provided for representing the non-convergent part of the geometrical optics contribution to the RCS of an arbitrary uniform straight ergodic chaotic duct illuminated by a plane wave. The RCS is a random function which appears to have the same characteristics, for a given angle of incidence, as a converged geometrical optics or modal solution at sufficiently high frequencies. The random wave model for monostatic scattering is probably not as accurate, but still provides good predictions of the mean RCS and lobing rate.

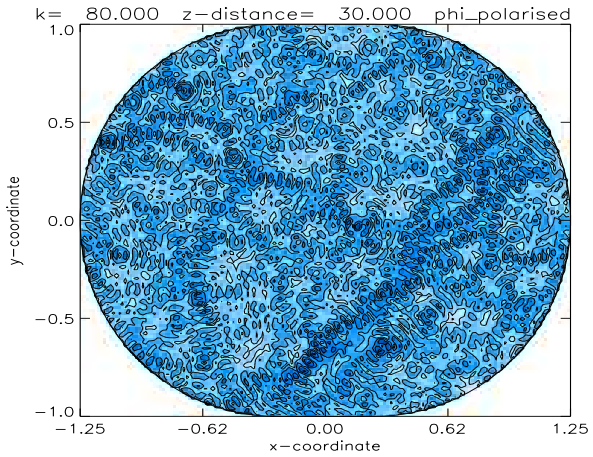

Figure 2. *Field magnitude, random waves, ensemble member 1.*

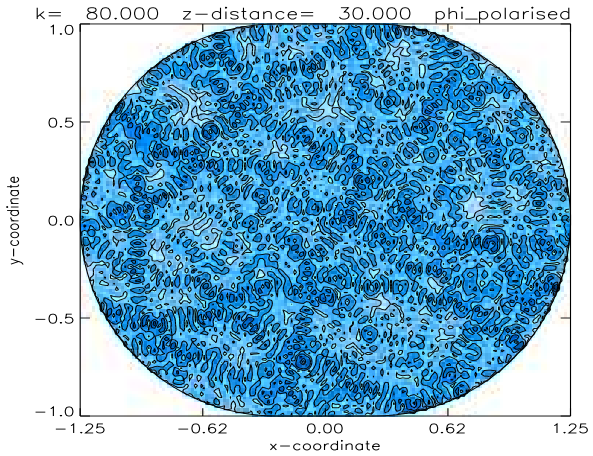

Figure 3. *Field magnitude, random waves, ensemble member 2.*

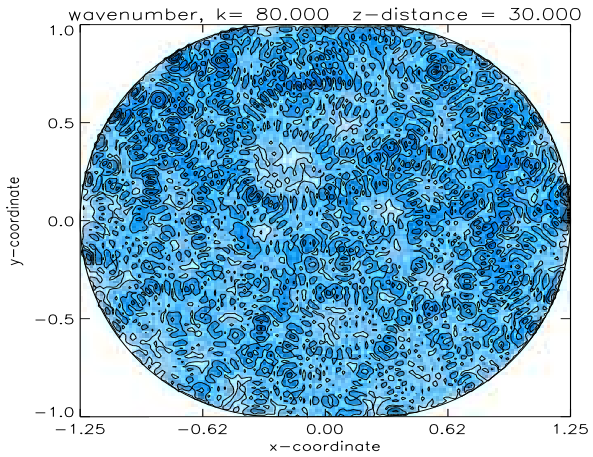

Figure 4. *Field magnitude, modal solution.*

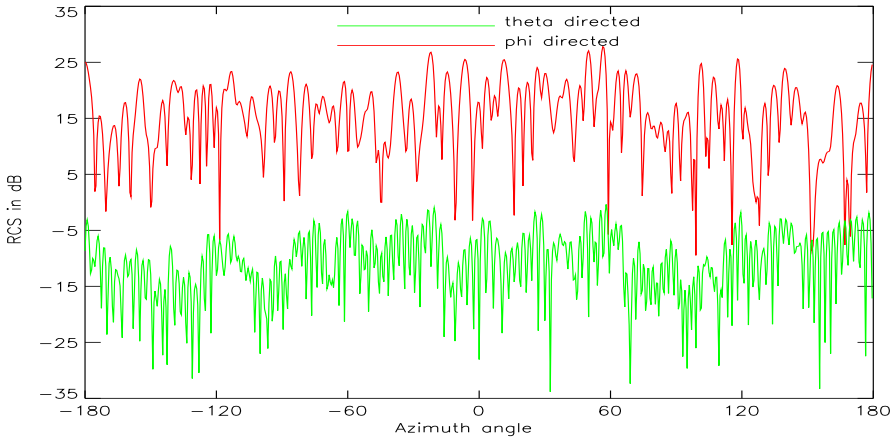

Figure 5. *RCS, random waves, ensemble member 1.*

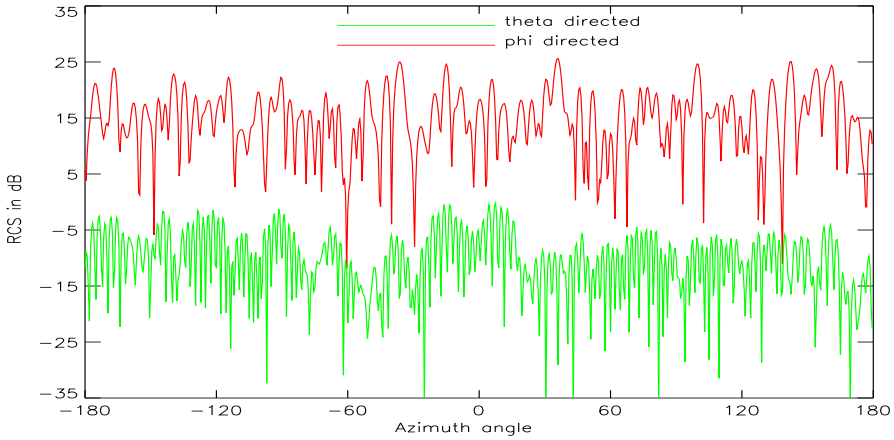

Figure 6. *RCS, random waves, ensemble member 2.*

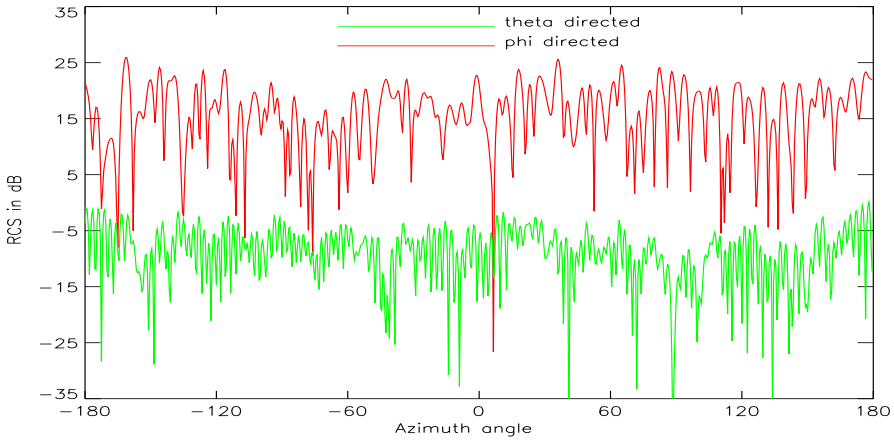

Figure 7. *RCS, reference modal solution.*

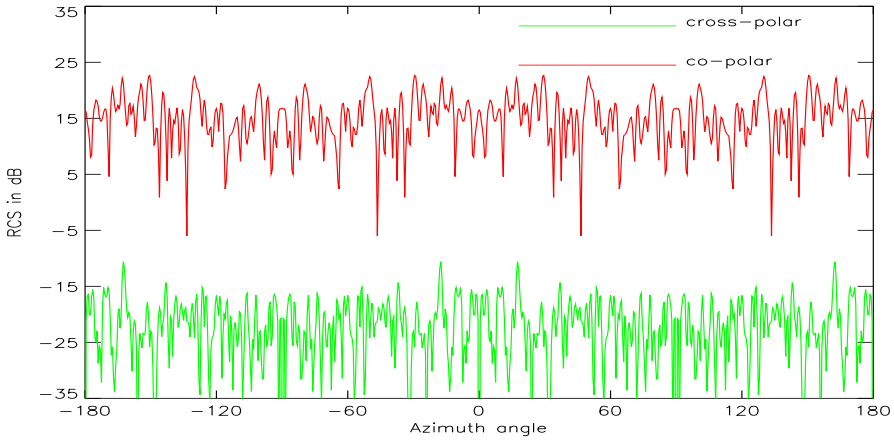

Figure 8. *RCS, random waves, ensemble member 1.*

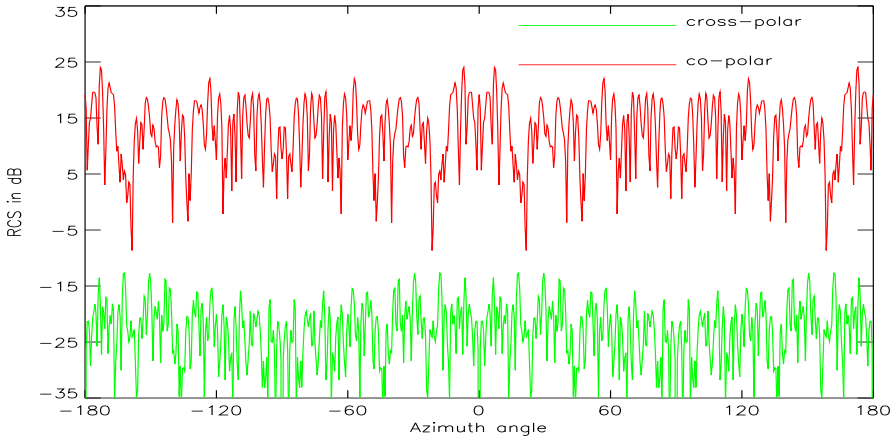

Figure 9. *RCS, random waves, ensemble member 2.*

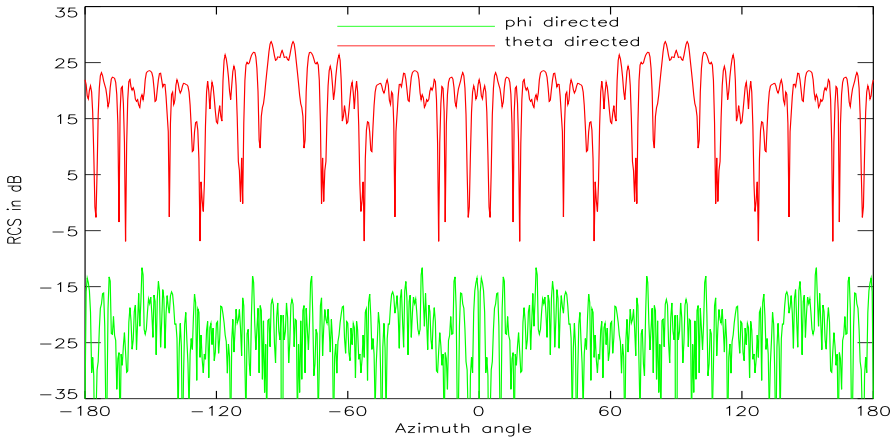

Figure 10. *RCS, reference modal solution.*

References

[1] A.J.MACKAY *'Chaos theory and first order ray tracing in ducts'*, IEE Electronics Letters, Vol 34, No. 14, pp1388-1389, July 1998.

[2] A.J.MACKAY *'Application of chaos theory to ray tracing in ducts'*, IEE Proceedings Radar Sonar and Navigation, vol 146, No. 6, pp298-304, December 1999.

[3] A.J.MACKAY *'Chaos theory applied to first order ray tracing in ducts'* DERA report number DERA/SN/R/TR980002/1.0, DERA Malvern, St Andrew's Road, Great Malvern, Worcs, WR14 3PS, UK. (Available through DRIC) April 1998.

[4] A.J.MACKAY *'New representations of ray tracing, chaos theory and random waves in straight ducts'* DERA report number DERA/S&P/RAD/CR990108/1.0, DERA Malvern, St Andrew's Road, Great Malvern, Worcs, WR14 3PS, UK. (Available through DRIC) March 1999.

[5] G.A.DESCHAMPS, *Ray techniques in electromagnetics*, Invited paper, Proceedings of the IEEE, Vol. 60, No. 9, pp 1022-1035, September 1972.

[6] J.M.SONG, C.C.LU, W.C.CHEW, S.W.LEE *Fast Illinois Solver Code (FISC)*, IEEE Antennas and Propagation Magazine, Vol 40, No 3, June 1998, pp27-33.

[7] M.C.GUTZWILLER, *Chaos in classical and quantum mechanics*, Springer-verlag, Interdisciplinary Appled Mathematics series, 1990.

[8] M.V.BERRY, J.P.KEATING, H.SCHOMERUS, *Universal twinkling exponents for spectral fluctuations associated with mixed chaology*, Proc. R. Soc. Lond. A 456, pp1659-1668, 2000.

[9] J.P.KEATING, S.D.PRADO, *Orbit bifurcations and the scarring of wavefunctions*, accepted for publication in Proc. R. Soc. Lond. A, 2001.

[10] L.MANDEL, E.WOLF, *Optical coherence and quantum optics*, Cambridge University Press, 1995.

[11] E.B.BOGOMOLNY, *Smoothed wavefunctions of chaotic quantum systems*, Physica D 31, pp169-189, 1988.

[12] R.J.BURKHOLDER, R.C.CHOU, P.H.PATHAK, *Two ray shooting methods for analysing the EM scattering by large open-ended cavities.* Computer Physics Communications (North Holland), Vol 68, (pp 353-365), 1991.

[13] T.S.M.MACLEAN, *Principles of antennas: wire and aperture*, Cambridge University Press, section 11.4, 1986.

[14] A.J.MACKAY *'The modal analysis and RCS prediction of circular and general cross section straight ducts'* DERA report number DERA/S&P/RAD/TR990315/1.0, DERA Malvern, St Andrew's Road, Great Malvern, Worcs, WR14 3PS, UK. (Available through DRIC) June 1999.